

## Nonlinear Analysis for Control of Xenon Oscillations using Sigmoid Functions

Abhishek Chakraborty<sup>1</sup>, Suneet Singh<sup>2</sup>

<sup>1</sup>Nuclear Power Corporation of India Limited, Anushaktinagar, Mumbai: 400094, India, abhishekc@npcil.co.in

<sup>2</sup>Department of Energy Science and Engineering, IIT Bombay, Mumbai: 400076, India, suneet.singh@iitb.ac.in

**Abstract** - Xenon oscillations are very important for designing nuclear reactors operating in the thermal energy spectrum. The nature of the power oscillations depend on the size of the reactor and the flux level of operation. The larger the size of reactor and higher the flux level of operation, more the reactor is susceptible to xenon oscillations. Control strategies have to be designed in order to suppress the growth of xenon oscillations. One possible choice of modeling a control function can be "clipping" at some threshold level. The effect of "clipping" cannot be included in the linear stability analysis since it is a discontinuous function and hence the estimation of the Jacobian is difficult. However, the "clipping" can be modeled using "sigmoid" functions. Also, the selection of sigmoid function and its parameters will affect the evaluation of the stability of the system. The nonlinear analysis for control of xenon oscillations using sigmoid functions has been performed in this work. The hyperbolic tangent function (a type of sigmoid function) has been used for modeling of the control action to suppress the growth of the perturbation. The method has been applied to a one dimensional homogenous slab reactor to present a "proof of principle". The effect of different parameters of the sigmoid function on the stability of xenon oscillations has been studied.

## I. INTRODUCTION

### 1. Background

Oscillation in reactor power due to the variation of xenon has been of deep interest for reactor physicists from the beginning. The effects of xenon are a potential source of instability in nuclear reactors operating in thermal spectrum. The instantaneous production rate of Xenon-135 depends upon the Iodine-135 concentration, and, hence upon the local neutron flux history. On the other hand, the removal of Xe-135 depends on the instantaneous flux through the neutron absorption process and upon the flux history through the Xe-135 decay process. Xenon oscillations are produced by the delay between xenon burnup and xenon buildup from iodine decay. An oscillatory regime in reactor power can be established which can cause the power limits to exceed the allowable limits. A lot of work has been done in the study of these oscillations and different control strategies have been designed for suppressing these oscillations.

The assessment of stability of xenon oscillations generally is carried out by numerical solution of the model equations under different reactivity perturbations and core irradiations as discussed by Chernick [1], Lellouche et.al[2], Kobayashi et.al [3], Parhizhari et.al [4], Gyorey [5].

### 2. Importance of Non linear Stability Analysis

Linear stability analysis of xenon oscillations has been carried out by Stacey [6], Canosa et.al [7]. Linear Stability analysis is valid for "small" perturbations and the system behaviour for "large" perturbations cannot be predicted by the linear stability analysis. The system might exhibit "unstable" periodic solutions on the stable side of the

stability boundary and "stable" periodic solutions on the unstable side. Hence, a detailed bifurcation analysis is required to estimate the "global" stability characteristics of the system. In the "hard" or sub-critical Hopf region, the equilibrium point is linearly stable but due to the existence of an unstable limit cycle about this point growing oscillations might be observed for large perturbations. This means that for a "sub-critical" Hopf bifurcation, the points which lie on the stable side of the linear stability boundary may become unstable for "large" perturbations. But for "soft" or supercritical Hopf bifurcations, the stable region of the stability boundary is globally stable but there exist stable limit cycles on the unstable side. Both types of bifurcations may exist for a system in different regions of parameter spaces, and hence the point where the cross-over takes place needs to be identified which can be only done by non-linear analysis methods.

The problem of space independent xenon oscillations was revisited by Rizwan-uddin [8] using the same model equations used by Chernick [1] with nonlinear analysis techniques. The existence of Hopf Bifurcation (both supercritical and subcritical) was observed in different parameter spaces. Expansion methods for estimating nonlinear stability domains were analyzed by Yang et.al [9]. The studies performed by Rizwan-uddin, Chernick and Yang deal with space independent xenon oscillations.

### 3. Objective of the Present Analysis

A possible model for control of these oscillations was demonstrated by Gyorey [10] where it is modeled as "clipping" of the amplitudes of the different higher harmonics above a certain threshold value. The effect of "clipping" cannot be included in the linear stability analysis since it is a discontinuous function and hence the estimation

of the Jacobian is difficult. "Clipping" can be modeled using "sigmoid" functions. However, the selection of sigmoid function and its parameters will also affect the evaluation of the stability of the system. In this paper, the effect of this kind, for out of phase xenon oscillations, in a homogeneous slab reactor has been carried out with the bifurcation code, "BIFDD"[11].

## II. MODEL EQUATIONS FOR XENON OSCILLATIONS

The model is based on that used by Gyorey [2] where modal expansion method is used for the solution of space time dependent neutron kinetics equations coupled with xenon and iodine equations. The neutron flux, iodine concentration and xenon concentration at any time are assumed to be written as summation of the steady state value and a small perturbation term,

$$\phi(\mathbf{r},t) = \phi_0(\mathbf{r}) + \delta\phi(\mathbf{r},t) \quad (1)$$

$$I(\mathbf{r},t) = I_0(\mathbf{r}) + \delta I(\mathbf{r},t) \quad (2)$$

$$X(\mathbf{r},t) = X_0(\mathbf{r}) + \delta X(\mathbf{r},t) \quad (3)$$

Equations (1),(2) and (3) can be substituted in the space time dependent neutron, xenon and iodine equations. The perturbation is expanded in terms of modes. Neglecting intermodal interaction terms, the final set of equations for each mode can be written as:

$$\Lambda_n \frac{dN_n}{dT} = -\Gamma_n [S_n N_n + F_{nn} X_n + \Psi_{nnn} N_n X_n] \quad (4)$$

$$\frac{dX_n}{dT} = \frac{\gamma_I}{\gamma} I_n + \left[ \frac{\gamma_X}{\gamma} - P_{nn} \right] N_n - [1 + F_{nn}] X_n - \Psi_{nnn} N_n X_n \quad (5)$$

$$\frac{dI_n}{dT} = \frac{\lambda_I}{\lambda_X} [N_n - I_n] \quad (6)$$

The details of these equations are given in Gyorey [2].

For a 1D homogenous bare slab reactor of width "H", the basis functions and the corresponding integrals become as follows:

$$\Psi_i = \sqrt{\frac{2}{H}} \text{Sin}\left(\frac{i\pi}{H} x\right), i = 2,3,\dots \quad (7)$$

$$F_{ij} = \Omega \frac{2}{\pi} \int_0^\pi \text{Sin } \theta \text{Sin}(i\theta) \text{Sin}(j\theta) d\theta \quad (8)$$

$$\Psi_{ijk} = \Omega \frac{2}{\pi} \int_0^\pi \text{Sin}(i\theta) \text{Sin}(j\theta) \text{Sin}(h\theta) d\theta \quad (9)$$

$$P_{ij} = \Omega \frac{2}{\pi} \int_0^\pi \frac{\text{Sin}(i\theta) \text{Sin}(j\theta) \text{Sin}(\theta)}{1 + \Omega \text{Sin } \theta} d\theta \quad (10)$$

where,

$$\theta = \frac{\pi}{H} x \text{ and } \Omega \equiv \frac{\sigma_x}{\lambda_x} \phi_0(\mathbf{max}).$$

## III. MODELING OF SPATIAL CONTROL

The spatial control mechanism in principle is designed to suppress the growth of these higher harmonics which would give distortions to the flux shape in the reactor core. As mentioned earlier, the control action can be modeled using "sigmoid" functions. Hyperbolic tangent function (tanh) has been used as a sigmoid function in this analysis.

Since,  $|N_m| \leq 1$ , the form of the control function, CF, is as follows:

$$CF = \frac{1}{C1} [\tanh(D(N_n + n_c)) - \tanh(D(N_n - n_c))] \quad (11)$$

The value of C1 is such that CF=1 at  $N_n = 0$

The plots of the control functions CF1 and CF2 for different values of D, C1 and  $n_c$  are given in Fig.1 and Fig.2 respectively. This function is multiplied with the R.H.S. of equation (4).

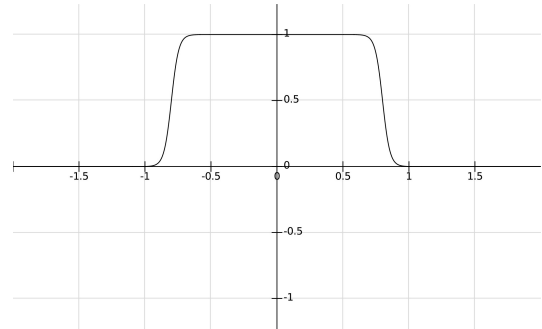


Fig. 1 CF1 with D = 18,  $n_c = 0.8$ , C1 = 2.0.

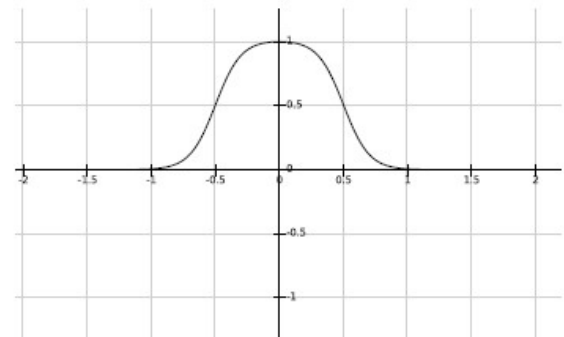


Fig. 2 CF2 with D = 5,  $n_c = 0.5$ , C1 = 1.97.

#### IV LINEAR STABILITY BOUNDARY - EIGENVALUE APPROACH

The equations (4)-(6) may be compactly represented in the form,

$$\frac{d\vec{Y}(t)}{dt} = F(\vec{Y}(t), \Omega, S_n) \quad (12)$$

where  $\vec{Y} = (N_n, I_n, X_n)$  is a three component vector.

The fixed points or the equilibrium points of the system satisfy the equation

$$F(\vec{Y}_e, \Omega, S_n) = 0 \quad (13),$$

The stability analysis involves a slight perturbation of the system around a chosen equilibrium point. Let  $\vec{Y}_d$  be the perturbation around it, then equation (12) leads to the following equation in perturbation variable  $\vec{Y}_d$ .

$$\frac{d\vec{Y}_d(t)}{dt} = F \left\{ \vec{Y}_e + \vec{Y}_d(t), \Omega, S_n \right\} \quad (14)$$

Expanding (14) in Taylor series and neglecting higher powers ( $\geq 2$ ) of  $\vec{Y}_d$  (i.e., for small values of  $\vec{Y}_d$ ), the linearized version of the basic evolutionary equation is arrived at.

The eigenvalue spectrum of the associated Jacobian matrix evaluated at the equilibrium points gives the nature of the system behaviour in the neighborhood of the equilibrium point.

The values of parameters at which the eigenvalue(s) of the Jacobian become purely imaginary are chosen as the stability boundary.  $P_{ij}$ ,  $F_{ij}$  and  $\Psi_{ij}$  are functions of  $\Omega$ . Here,  $S_n$  and  $\Omega$  are chosen as the bifurcating parameters and the values at which the eigenvalues become purely imaginary are found out. Basically,  $S_n$  depends on the geometry and  $\Omega$  depends on the flux level of operation. For a homogeneous slab reactor,  $S_n$  can be written as [10]

$$S_n = \frac{1.03}{0.03} \frac{M^2}{H^2} (n^2 - 1) \quad (15)$$

Bifurcation analysis has been performed using the code "BIFDD" for first and second harmonic with control. The stability of these periodic solutions is governed by the parameter  $\beta$  (different from the delayed neutron fraction) which can be expanded in the powers of a small parameter  $\varepsilon$  as follows (Rizwanuddin [12])

$$\beta = \varepsilon\beta_1 + \varepsilon^2\beta_2 + \dots \quad (16)$$

The value of  $\beta_1$  is found to be zero, hence the value of  $\beta_2$  indicates the stability of the periodic solutions.  $\beta_2 > 0$  indicates subcritical Hopf Bifurcation,  $\beta_2 < 0$  indicates supercritical Hopf Bifurcation.  $\beta_2$  has been estimated by the code "BIFDD". If the oscillations on the stable side of the stability boundary die down for "small" perturbations and grow for "large" perturbations, then it is called sub-critical Hopf Bifurcation. If the oscillations grow and settle down on a limit cycle on the unstable side then it is called a supercritical Hopf Bifurcation. This can be seen from Fig.3.

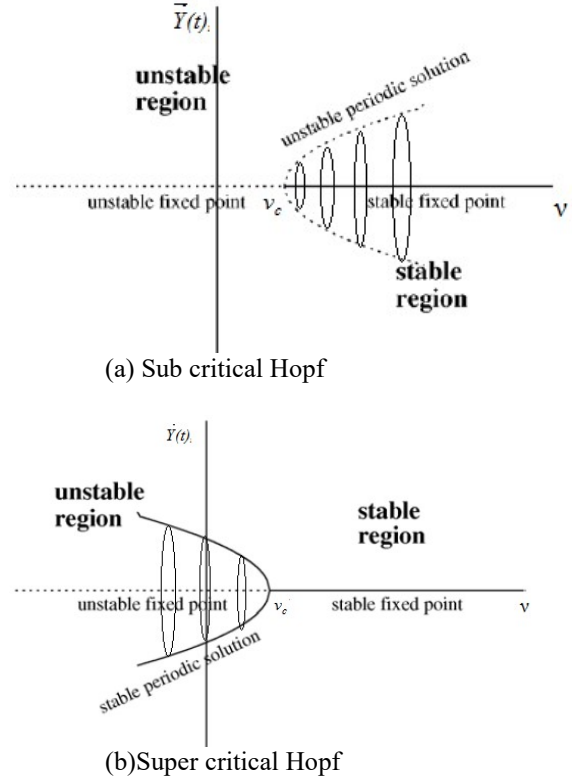


Fig. 3 Subcritical and Supercritical Hopf Bifurcation

#### V RESULTS

For a given geometry, the value of  $S_n$  is fixed.  $\Omega$  depends on the operating flux level, and the integrals  $F_{ij}$ ,  $\Psi_{ijm}$  and  $P_{ij}$  are functions of  $\Omega$  as shown in Eqns (10), (11) and (12). Hence,  $\Omega$  is varied from 0.25 to 30 and the stability boundary is estimated for first harmonic (2<sup>nd</sup> mode) and second harmonic (3<sup>rd</sup> mode). The stability boundaries for the second and 3rd mode are given in Figs. 3 and 4, respectively. It is worth mentioning that with this choice of control functions, the stability boundary remains unchanged.

In order to verify the stability boundary, numerical simulations are carried out at three points (a, b, c) about the stability boundary for both the modes using ODE23s

package of MATLAB. The parametric values of these points are given in Table 1.

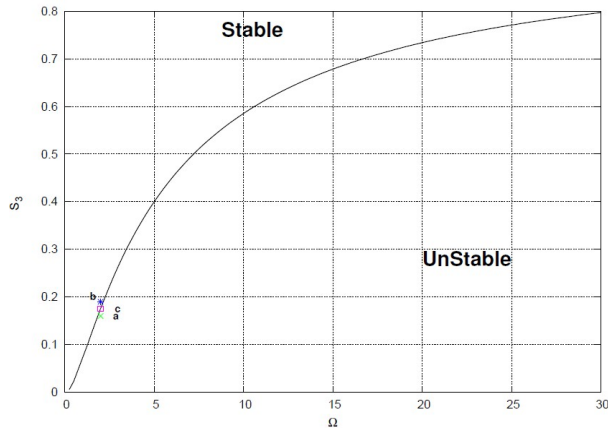


Fig. 4 Stability boundary for 2nd mode (first harmonic) in the  $S_2 - \Omega$  plane.

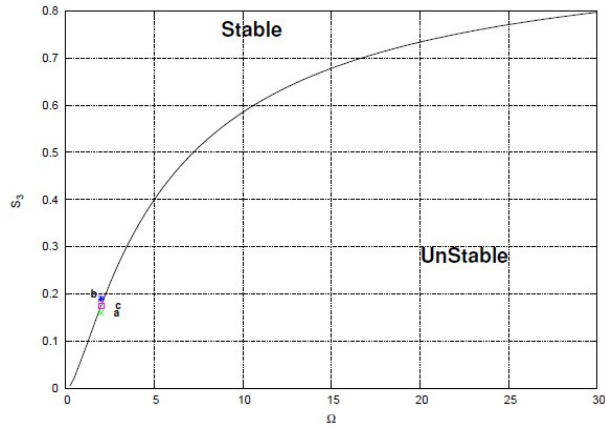


Fig. 5 Stability boundary for 3rd mode (second harmonic) in the  $S_3 - \Omega$  plane.

Table 1 Parametric values at which simulations have been carried out

		First Harmonic	Second Harmonic
		$\Omega=2.0$	
		$S_{2,crit}=0.187$	$S_{3,crit}=0.1754$
Point a	Unstable side	$S_2 = 0.17$	$S_3 = 0.16$
Point b	Stable Side	$S_2 = 0.195$	$S_3 = 0.19$
Point c	On the stability Boundary	$S_2 = 0.187$	$S_3 = 0.1754$

## 1. Numerical Simulations without considering Control Function

### a) Simulation for First Harmonic

The simulations at point "a" show growing oscillations since it lies on the unstable side of the stability boundary. This is given in Fig.6.

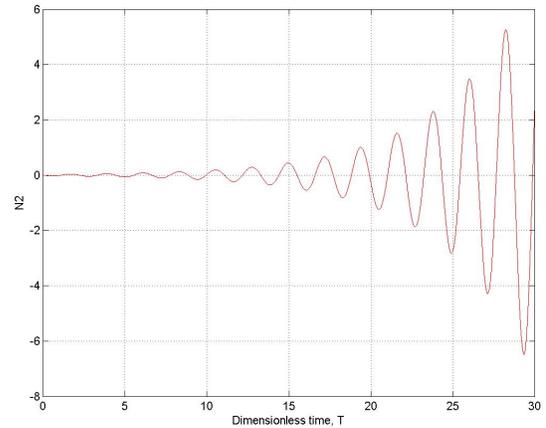


Fig. 6 Numerical Simulation at Point a (Unstable focus)

Similarly, solving the coupled ODEs at point "b", damped/decaying oscillations are observed since it lies on the stable side of the stability boundary as shown in Fig.6.

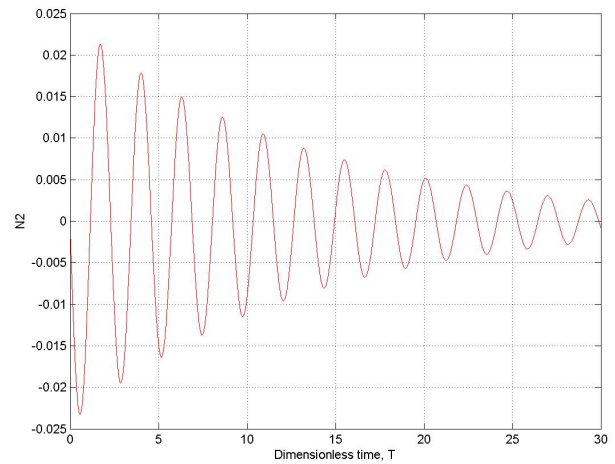


Fig. 7 Numerical Simulation at Point b (Stable focus)

Since, point "c" lies on the stability boundary, constant amplitude oscillations are observed as shown in Fig.8.

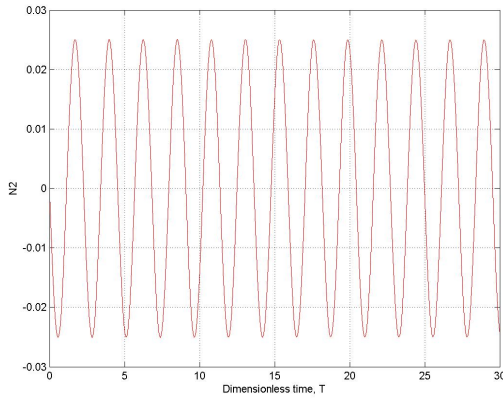


Fig. 8 Numerical Simulation at Point c (on the stability boundary)

### b) Simulation for Second Harmonic

Numerical simulations at points "a" and "c" show similar nature as that for the first harmonic. However, point "b" acts as a "stable focus" for small perturbations but acts as an "unstable focus" for large perturbations. This can be seen from the phase space plot given in Fig.9 that the "unstable limit cycle" repels all trajectories away from it.

Hence, there exists an unstable limit cycle about the stable fixed point which means that the equilibrium point acts as a stable focus for small perturbations and as an unstable focus for large perturbations. This is a characteristic of subcritical Hopf Bifurcation.

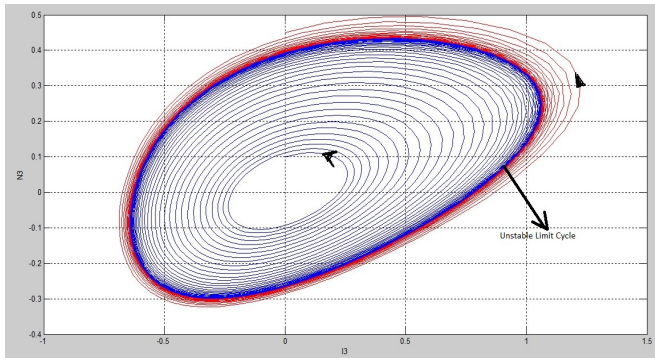


Fig. 9 Numerical Simulation at point "b" (on the stable side). (Blue color shows a stable focus, Red color shows an unstable focus)

## 2. Numerical Simulations considering Control Function

Numerical simulations were carried out for the second harmonic using both the control functions CF1 and CF2 at points "b" (stable side) and "a" (unstable side). It can be seen from Fig.10 and 11 that the point "b" acts as a stable

focus for small as well as large perturbations for CF1. Similar, behaviour is also observed for the control function CF2.

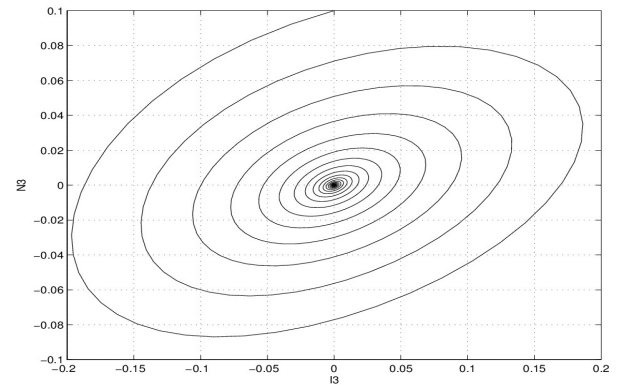


Fig. 10 Numerical Simulation at Point "b" for small perturbations for CF1 (Stable focus)

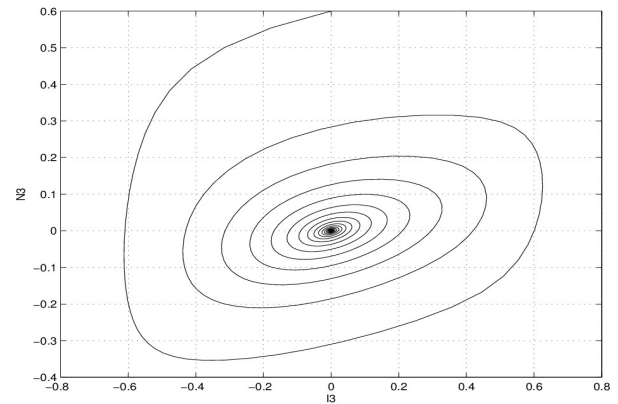


Fig. 11 Numerical Simulation at Point "b" for large perturbations for CF1 (Stable focus)

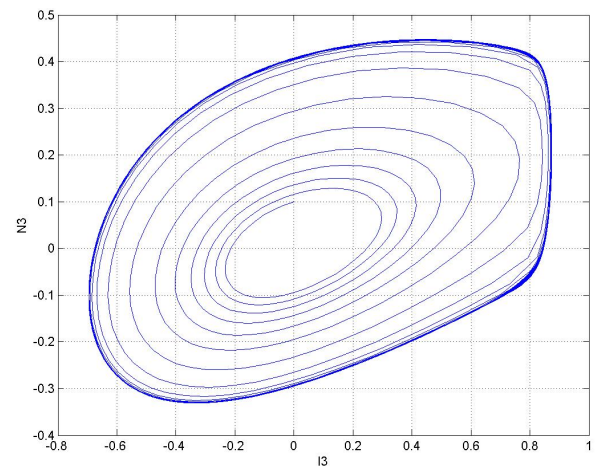


Fig. 12 Numerical simulation at point "a" for second harmonic using control function CF1.

Numerical simulations were also carried out for the second harmonic at point "a" which lies on the unstable side of the stability boundary for both the control functions CF1 and CF2. Stable limit cycles were observed on solution of the coupled ODEs for both the control functions and are shown in Fig.12 and 13.

This is a signature of supercritical Hopf Bifurcation. Using the Bifurcation code, BIFDD, the value of  $\beta_2$  was estimated for this range for both the control function (CF2) and also without control. The results are given in Fig.14.

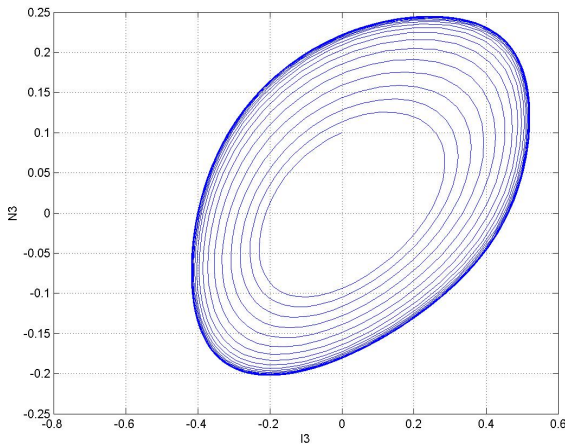


Fig. 13 Numerical simulation at point "a" for second harmonic using control function CF2.

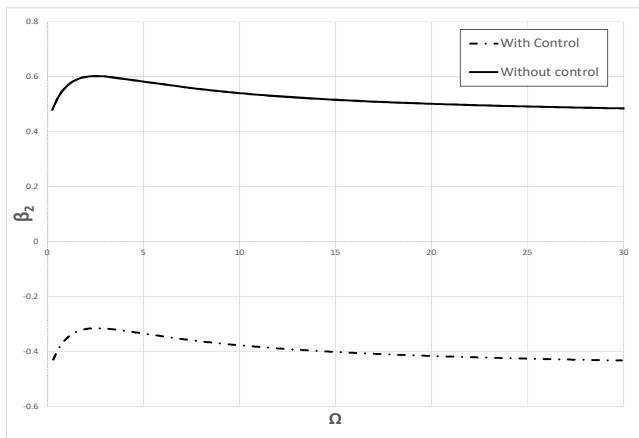


Fig. 14 Variation of  $\beta_2$  with control function with different  $\Omega$  for second harmonic.

It can be seen from Fig.14 that without the application of any control function, the value of  $\beta_2 > 0$ , which implies a

sub-critical Hopf Bifurcation. On the application of control function, CF2, the value of  $\beta_2$  is less than zero, which implies supercritical Hopf Bifurcation. The existence of supercritical Hopf Bifurcation on application of a control function has been verified earlier by numerically solving the equations. However, for the control function, CF1, the value of  $\beta_2$  is identical to that obtained for the case without any control function, even if the numerical simulations show a super critical Hopf bifurcation characteristic. This is due to the fact that the control function, CF1, is more "flat" than CF2. Hence, for capturing the effect of CF1, higher order terms have to be estimated (like  $\beta_4, \beta_6, \dots$ ).

Also, the amplitude of the stable limit cycles on the unstable side increase as one goes away from the stability boundary. For the second harmonic, for  $\Omega=2.0$ , the  $S_{3,crit}=0.1754$ . Hence, the simulations have also been carried out at  $S_3=0.175, 0.171$  and  $0.165$ , respectively (lying on the unstable side) for both the control functions CF1 and CF2 and the results are given in Fig.15 and 16 respectively.

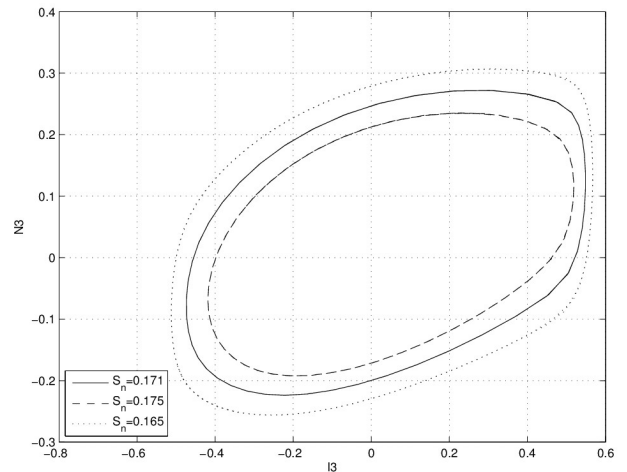


Fig. 15 Stable limit cycles on unstable side for CF1.

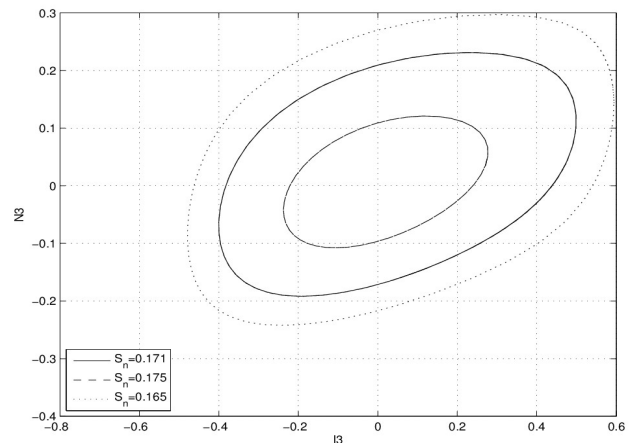


Fig. 16 Stable limit cycles on unstable side for CF2.

## VI CONCLUSIONS

The nonlinear analysis for control of xenon oscillations using sigmoid functions has been performed using the tool BIFDD. The hyperbolic tangent function has been used for modeling of the control action to suppress the growth of the perturbation. This has been applied to a one dimensional homogenous slab reactor to present a “proof of principle”. The effect of different parameters of the sigmoid function on the stability of xenon oscillations has been studied. It has been found that the effect of a control function is to convert a “sub-critical” Hopf Bifurcation to a “super critical” Hopf Bifurcation for the second harmonic. This approach for analyzing the stability of xenon oscillations with control can be extended to multipoint reactor kinetics to study the actual reactor systems like Pressurised Heavy Water Reactors and Pressurised Water Reactors.

## NOMENCLATURE

- $N_n$  = Normalised coefficient of the expansion functions for the  $n^{\text{th}}$  mode for neutron flux.  
 $X_n$  = Normalised coefficient of the expansion functions for the  $n^{\text{th}}$  mode for Xenon distribution.  
 $I_n$  = Normalised coefficient of the expansion functions for the  $n^{\text{th}}$  mode for Iodine distribution.  
 $S_n$  = Sub-criticality associated with  $n^{\text{th}}$  mode  
 $H$  = Width of the slab.  
 $\Psi_n$  = Orthogonal Basis Function for  $n^{\text{th}}$  mode.  
 $n_c$  = Cut off value of  $N_n$ .  
 $D$  = Slope of the sigmoid function.  
 $C1$  = Constant such that  $CF=1$  at  $N_n = 0$ .  
 $\vec{Y}_e$  = Equilibrium point for  $\mathbf{Y}$ .  
 $\gamma_i$  = The fission yield of Iodine -135  
 $\gamma_x$  = The fission yield of Xenon-135.  
 $\gamma$  = The net yield of Iodine -135 and Xenon-135.  
 $\sigma_x$  = Microscopic absorption cross-section of Xe-135.  
 $\lambda_i$  = Decay constant of I-135.  
 $\lambda_x$  = Decay Constant of Xe-135.  
 $\Lambda_n$  = Effective neutron generation time for  $n^{\text{th}}$  mode. (s)  
 $CF$  = Control Function

## REFERENCES

1. CHERNICK, J. The Dynamics of a Xenon-Controlled Reactor. *Nuclear Science and Engineering* **8**, 233–243 (1960).
2. LELLOUCHE, G. S. Space Dependent Xenon Oscillations. *Nuclear Science and Engineering* **12**, 482–489 (1962).
3. KOBAYASHI, K. & YOSHIKUNI, M. Analysis of

- Xenon Oscillation by Coupled Reactor Model. *Journal of Nuclear Science and Technology* **19**, 107–118 (1982).
4. PARHIZKARI, H., AGHAIE, M., ZOLFAGHARI, A. & MINUCHEHR, A. An approach to stability analysis of spatial xenon oscillations in WWER-1000 reactors. *Annals of Nuclear Energy* **79**, 125–132 (2015).
5. GYOREY, G. L. The Effect of Modal Interaction in the Xenon Instability Problem. *Nuclear Science and Engineering* **13**, 338–344 (1962).
6. STACEY, W. M. *Nuclear Reactor Physics*. (2007). doi:10.1002/9783527611041
7. CANOSA, J. & BROOKS, H. Xenon-Induced Oscillations. *Nuclear Science and Engineering* **26**, 237–253 (1966).
8. RIZWAN-UDDIN. Non-linear dynamics of space-independent xenon oscillations. *Dynamics and Stability of Systems* **10**, 33–48 (1995).
9. YANG, C. Y. & CHO, N. Z. Expansion Methods for finding non linear stability domains of nuclear reactor models. *Annals of Nuclear Energy* **19**, 347–368 (1992).
10. GYOREY, G. L. On the theory of xenon induced instabilities in neutron flux distribution. (The University of Michigan, 1960).
11. HASSARD, B. *Theory and Applications of Hopf Bifurcation*. (Cambridge University Press, 1981).
12. RIZWAN-UDDIN. Turning points and sub- and supercritical bifurcations in a simple BWR model. *Nuclear Engineering and Design* **236**, 267–283 (2006).